The Dispersion Properties of Three-dimensional Magnetized Plasma Photonic Crystals as the Mixed Polarized Waves Considered

Hai-Feng Zhang[1,2], **Yi-Bing Lin**[2], **Yu-Qing Chen**[2], **and Guo-Wen Ding**[1]

[1]College of Electronic and Information Engineering
Nanjing University of Aeronautics and Astronautics, Nanjing 210016, China
[2]Nanjing Artillery Academy, Nanjing 211132, China

Abstract— In this paper, the dispersion properties of three-dimensional (3D) magnetized plasma photonic crystals (MPPCs) with face-centered-cubic (fcc) lattices are theoretically investigated based on the modified plane wave expansion (PWE) method, in which the homogeneous magnetized plasma spheres are immersed in the homogeneous and isotropic dielectric background, as the mixed polarized waves and magneto-optical Voigt effects are considered. The more general case has been studied, and the photonic band gap (PBG) of such MPPCs is not only for the left and right circular polarized waves but also for the mixed polarized waves. The equations for calculating the PBG for all of the electromagnetic waves in such 3D MPPCs also are theoretically deduced. Theoretical computing results show that one PBG and two flatbands regions can be observed. Compared to the conventional dielectric-air photonic crystals with similar structure, the larger PBG can be obtained in such 3D MPPCs. However, the narrower PBG can be achieved compared to the PBG for the extraordinary mode, but the larger upper edge frequency of flatbands region can be obtained.

1. INTRODUCTION

In 2004, the concept of plasma photonic crystals (PPCs) is firstly proposed by Hojo and coworker [1]. Compared to the conventional dielectric PCs, the PPCs can display the strong spatial dispersion [1] since the physical properties of plasma can be easily tuned by many parameters, such as the plasma density, the temperature of electron and the external magnetic field [2]. If the external magnetic field is introduced into the PPCs, the magnetized plasma photonic crystals (MPPCs) can be obtained. Compared to the PPCs, the more complicated EM modes can be found in the MPPCs [2]. If the external magnetic field is perpendicular to the EM wave vector, the Voigt effects can be observed in the magnetized plasma [2]. In this configuration, two basic EM modes can be found [2], which are named the extraordinary and ordinary modes, respectively. If the external magnetic field is parallel to the EM wave vector, the magneto-optical Faraday effects can be obtained. Therefore, the MPPCs become a new research field. Up to the present, a lot of reports on the MPPCs have been published. Especially, one- and two-dimensional (2D) MPPCs and PPCs have been investigated in detail [3–8]. However, there are a few reports of 3D PPCs and MPPCs until Zhang et al. [9–14] studied the dispersive properties of 3D PPCs and MPPCs. Compared to the 1D and 2D PCs, the 3D case can produce the complete PBGs and may be closer to the real applications. However, all of the reports on 3D MPPCs only focused on the dispersive properties of one kind of EM modes, which is the extraordinary mode for the Voigt effects or the right circular polarized wave for Faraday effects. In those reports, not all of the EM modes in 3D MPPCs are considered. Especially, the properties of mixed polarized modes in 3D MPPCs are not investigated. As mentioned above, the aims of this paper are to investigate the properties of PBG and surface plasmon modes in the 3D MPPCs with face-centered-cubic (fcc) lattices, which are composed of the homogeneous magnetized plasma spheres inserted in the dielectric background by the modified plane wave expansion (PWE) method, as the Voigt effects are considered.

2. THEORETICAL MODEL AND NUMERICAL METHOD

As shown in Fig. 1(a), we consider the radius of the sphere and lattice constant are R and a respectively; the relative dielectric function for magnetized plasma and dielectric background are ε_p and ε_a, respectively. We assume the incidence EM wave vector $\mathbf{k}$ is perpendicular to the external magnetic field $\mathbf{B}$ at any time (the Voigt effects of magnetized plasma are considered). As shown in Fig. 1(b). The high symmetry points for the fcc lattices have the coordinate as $X = (2\pi/a, 0, 0)$, $U = (2\pi/a, 0.5\pi/a, 0.5\pi/a)$, $L = (\pi/a, \pi/a, \pi/a)$, $\Gamma = (0, 0, 0)$, $W = (2\pi/a, \pi/a, 0)$ and $K = (1.5\pi/a, 1.5\pi/a, 0)$. It is well known that the expression of the relative dielectric function ε_p is

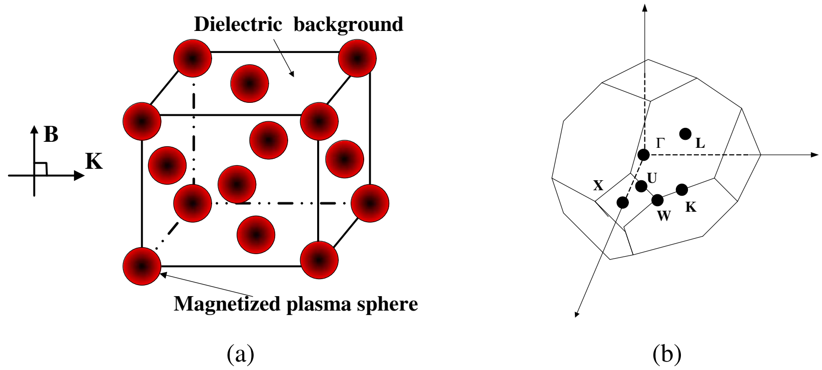

Figure 1: Schematic structure of 3D MPPCs with fcc lattices. (a) 3D MPPCs structure, and (b) the first irreducible Brillouin zone showing symmetry point used for computing the PBG.

determined by the angle between the wave vector and the external magnetic field [2]. Thus, the effective dielectric function ε_p can be written as [2]:

$$\boldsymbol{\varepsilon}_{\mathbf{p}}(\omega) = \begin{pmatrix} 1-\frac{\omega_p^2(\omega+j\nu_c)}{\omega[(\omega+j\nu_c)^2-\omega_c^2]} & 0 & \frac{-j\omega_p^2\omega_c}{\omega[(\omega+j\nu_c)^2-\omega_c^2]} \\ 0 & 1-\frac{\omega_p^2}{\omega(\omega+j\nu_c)} & 0 \\ \frac{j\omega_p^2\omega_c}{\omega[(\omega+j\nu_c)^2-\omega_c^2]} & 0 & 1-\frac{\omega_p^2(\omega+j\nu_c)}{\omega[(\omega+j\nu_c)^2-\omega_c^2]} \end{pmatrix} \tag{1}$$

In this expression, ω_p, ν_c, ω_c and ω are the plasma frequency, the electron collision frequency, plasma cyclotron frequency and the angular frequency, respectively. According to the PWE method, the dispersion properties of such MPPCs can be obtained by computing the flowing following equation,

$$\zeta^8\overleftrightarrow{\mathbf{I}} - \zeta^7\overleftrightarrow{\mathbf{X}}_7 - \zeta^6\overleftrightarrow{\mathbf{X}}_6 - \zeta^5\overleftrightarrow{\mathbf{X}}_5 - \zeta^4\overleftrightarrow{\mathbf{X}}_4 - \zeta^3\overleftrightarrow{\mathbf{X}}_3 - \zeta^2\overleftrightarrow{\mathbf{X}}_2 - \zeta\overleftrightarrow{\mathbf{X}}_1 - \overleftrightarrow{\mathbf{X}}_0 = 0 \tag{2}$$

where

$$\begin{aligned}
\overleftrightarrow{\mathbf{X}}_7(\mathbf{G}|\mathbf{G}') &= -3j\frac{\nu_c}{c}\boldsymbol{\delta}_{\mathbf{G}\cdot\mathbf{G}'}, \quad \overleftrightarrow{\mathbf{X}}_6(\mathbf{G}|\mathbf{G}') = \frac{\left(2\nu_c^2+\omega_p^2+A\right)}{c^2}\boldsymbol{\delta}_{\mathbf{G}\cdot\mathbf{G}'} + \overleftrightarrow{\mathbf{M}}_{\mathbf{1}} + \overleftrightarrow{\mathbf{M}}_{\mathbf{2}} + \overleftrightarrow{\mathbf{M}}_{\mathbf{3}} + \overleftrightarrow{\mathbf{M}}_{\mathbf{4}}, \\
\overleftrightarrow{\mathbf{X}}_5(\mathbf{G}|\mathbf{G}') &= \frac{j\left(4\nu_c\omega_p^2+A\cdot\nu_c\right)}{c^3}\boldsymbol{\delta}_{\mathbf{G}\cdot\mathbf{G}'} + 3j\frac{\nu_c}{c}\cdot\left(\overleftrightarrow{\mathbf{M}}_{\mathbf{1}} + \overleftrightarrow{\mathbf{M}}_{\mathbf{2}} + \overleftrightarrow{\mathbf{M}}_{\mathbf{3}}\right), \\
\overleftrightarrow{\mathbf{X}}_4(\mathbf{G}|\mathbf{G}') &= \frac{-\left(2\nu_c^2\omega_p^2+\omega_p^4+A\cdot\omega_p^2\right)}{c^4}\boldsymbol{\delta}_{\mathbf{G}\cdot\mathbf{G}'} - \frac{\left(2\nu_c^2+\omega_p^2+A\right)}{c^2}\cdot\overleftrightarrow{\mathbf{M}}_{\mathbf{1}} - \frac{\left(2\nu_c^2+\omega_p^2+B\right)}{c^2}\overleftrightarrow{\mathbf{M}}_{\mathbf{2}} \\
&\quad -\frac{\left(2\nu_c^2+A\right)}{c^2}\overleftrightarrow{\mathbf{M}}_{\mathbf{3}}, \\
\overleftrightarrow{\mathbf{X}}_3(\mathbf{G}|\mathbf{G}') &= \frac{-3j\nu_c^2\omega_p^4}{c^5}\boldsymbol{\delta}_{\mathbf{G}\cdot\mathbf{G}'} - j\frac{\left(4\nu_c\omega_p^2+A\cdot\nu_c\right)}{c^3}\cdot\overleftrightarrow{\mathbf{M}}_{\mathbf{1}} - j\frac{\left(3\nu_c\omega_p^2+B\cdot\nu_c\right)}{c^3}\overleftrightarrow{\mathbf{M}}_{\mathbf{2}} \\
&\quad -j\frac{\left(2\nu_c\omega_p^2+A\cdot\nu_c\right)}{c^3}\overleftrightarrow{\mathbf{M}}_{\mathbf{3}} + j\frac{\omega_c\omega_p^2}{c^3}\overleftrightarrow{\mathbf{M}}_{\mathbf{4}}, \\
\overleftrightarrow{\mathbf{X}}_2(\mathbf{G}|\mathbf{G}') &= \frac{\omega_p^6}{c^6}\boldsymbol{\delta}_{\mathbf{G}\cdot\mathbf{G}'} + \frac{\left(2\nu_c^2\omega_p^2+\omega_p^4+A\cdot\omega_p^2\right)}{c^4}\cdot\overleftrightarrow{\mathbf{M}}_{\mathbf{1}} + \frac{\left(\nu_c^2\omega_p^2+B\cdot\omega_p^2\right)}{c^4}\overleftrightarrow{\mathbf{M}}_{\mathbf{2}} \\
&\quad +j\frac{\left(2\nu_c^2\omega_p^2+\omega_p^4\right)}{c^4}\overleftrightarrow{\mathbf{M}}_{\mathbf{3}} - \frac{\nu_c\omega_c\omega_p^2}{c^4}\overleftrightarrow{\mathbf{M}}_{\mathbf{4}}, \\
\overleftrightarrow{\mathbf{X}}_1(\mathbf{G}|\mathbf{G}') &= j\frac{3\nu_c\omega_p^4}{c^5}\cdot\overleftrightarrow{\mathbf{M}}_{\mathbf{1}} + j\frac{\nu_c\omega_p^4}{c^5}\overleftrightarrow{\mathbf{M}}_{\mathbf{2}} + j\frac{\nu_c\omega_p^4}{c^5}\overleftrightarrow{\mathbf{M}}_{\mathbf{3}} - j\frac{\omega_c\omega_p^4}{c^5}\overleftrightarrow{\mathbf{M}}_{\mathbf{4}}, \quad \overleftrightarrow{\mathbf{X}}_0(\mathbf{G}|\mathbf{G}') = -\frac{\omega_p^6}{c^6}\overleftrightarrow{\mathbf{M}}_{\mathbf{1}},
\end{aligned}$$

The parameters of Eq. (2) can be found in Ref. [15].

3. NUMERICAL RESULTS AND DISCUSSION

Without loss of generality, we use $\omega a/2\pi c$ to normalize the frequency region. We use a variable $\omega_{p0} = 2\pi c/a$ to define the plasma frequency, the plasma collision frequency and the plasma cyclotron frequency, as $\omega_p = 0.35\omega_{p0}$, $\omega_{pl} = 0.15\omega_{p0}$, $\nu_c = 0.02\omega_{pl}$ and $\omega_c = 0.6\omega_{pl}$, respectively. Obviously, ω_{p0} and ω_{pl} are the symbols to define the constants and have not any physical meanings. We also consider $\mu_a = 1$, and $\mu_p = 1$, respectively. In our calculation, we use 729 plane waves to make the convergence accuracy is better than 1% for the lower bands [9].

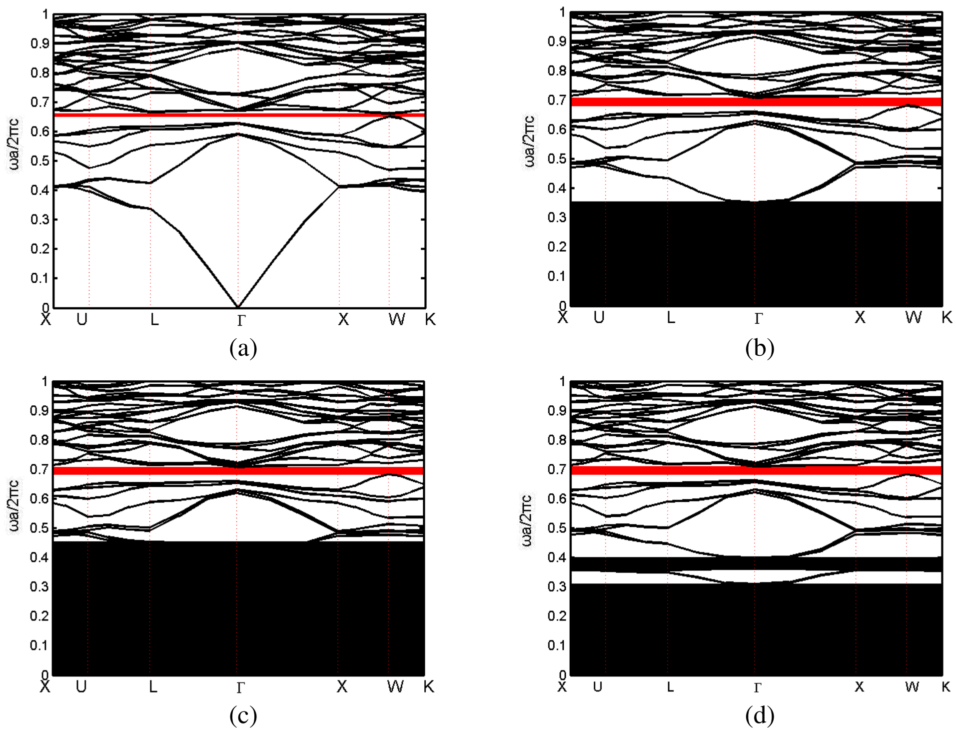

Figure 2: The band structures for such 3D MPPCs with $\varepsilon_a = 13.9$ and $f = 0.63$ but with different ω_p, ν_c and ω_c. (a) $\omega_p = \nu_c = \omega_c = 0$; (b) $\omega_p = 0.35\omega_{p0}$, $\nu_c = 0.02\omega_{pl}$ and $\omega_c = 0$; (c) $\omega_p = 0.35\omega_{p0}$, $\nu_c = 0.02\omega_{pl}$ and $\omega_c = 0.6\omega_{pl}$; (d) the band structures for the extraordinary mode in such 3D MPPCs with same parameters as Fig. 1(c). The red shaded regions indicate the PBGs.

As shown in Fig. 2(a), if $\omega_p = \omega_c = \nu_c = 0$, the magnetized plasma spheres can be looked as the air, and one complete PBG can be observed, which can be found at 0.6515–0.6611 $(2\pi c/a)$. If $\omega_p = 0.35\omega_{p0}$, $\nu_c = 0.02\omega_{pl}$, $\omega_c = 0$, the inserted spheres can be looked as the plasma, and a complete PBG and a flatbands region can be obtained. Obviously, the edges of PBG shift to higher frequency region. In this case, the PBG is located at 0.6808–0.7074 $(2\pi c/a)$. Compared to the results in Fig. 2(a), the bandwidth of PBG is enlarged obviously. The flatbands can be observed in the flatbands region, which spans from 0 to 0.35 $(2\pi c/a)$. The existence of surface plasmon modes produces the flatbands region. Fig. 2(c) demonstrates that, if the external magnetic field is introduced (Voigt effects are considered), one flatbands region can be obtained. The PBG also can be found at 0.6814–0.7067 $(2\pi c/a)$, whose edges shift to higher frequency region. The upper edge frequency of flatbands region is 0.4499 $(2\pi c/a)$. Compared to Fig. 2(a), the bandwidth of PBG is enhanced, which is 0.0253 $(2\pi c/a)$. Obviously, in Fig. 2(c), the PBG is for all of the EM modes (including the mixed polarized modes) in such 3D MPPCs. As a comparison, in Fig. 2(d), we plot the band structures for extraordinary mode in such 3D MPPCs with similar parameters as mentioned in Fig. 2(c). As shown in Fig. 2(d), one PBG and two flatbands regions can be obtained. The PBG runs from 0.6819 to 0.7082 $(2\pi c/a)$, and bandwidth is 0.0263 $(2\pi c/a)$. Two flatbands regions are located at 0–0.3072 $(2\pi c/a)$ and 0.361–0.3971 $(2\pi c/a)$, respectively. As we know, the upper edge frequencies of two flatbands regions and the lower edge of second flatbands region are nearly corresponding to the cutoff frequencies for left and the right circular polarization, and the upper hybrid frequency, respectively. Compared Fig. 2(c) to Fig. 2(d), the frequency range of PBG is narrowed, and only one flatbands region can be observed. The upper edge of flatbands region is upward to higher frequency region. It is noticed that Fig. 2(b) is the band structures for the ordinary mode in such 3D MPPCs. Compared to Fig. 2(c), the PBG for ordinary mode has a larger bandwidth. As mentioned above, the PBG for all of the EM modes in such 3D MPPCs can be achieved as the Voigt effects of magnetized plasma are considered, and the larger PBG can be obtained compared to the conventional isotropic 3D dielectric-air PCs with similar structure. Compared to band structures for the extraordinary and ordinary modes, the PBG for all of the EM modes has a narrower bandwidth, and only one flatbands region can be found. Here, we only focus on the first PBG in the frequency domain 0–$2\pi c/a$.

4. CONCLUSIONS

In summary, the properties of PBG and surface plasmon modes in the 3D MPPCs with fcc lattices are theoretically investigated based on the modified PWE method, in which the homogeneous magnetized plasma spheres are immersed in the homogeneous dielectric background, as the Voigt effects of magnetized plasma are considered (the incidence electromagnetic wave vector is perpendicular to the external magnetic field at any time). The equations for calculating the PBG for all of the EM modes in such 3D MPPCs are theoretically deduced. Based on the calculated results, some conclusions can be drawn. Compared to the conventional dielectric-air PCs, the larger PBG and one flatbands region can be obtained as the magnetized plasma is introduced. It is worth to be noticed that such PBG is not only for the extraordinary and ordinary modes but also can prohibit the mixed polarized modes. The flatbands are caused by the existence of surface plasmon modes which stem from the coupling effects between the magnetized plasma spheres.

ACKNOWLEDGMENT

This work was supported by the National Natural Science Foundation of China (Grant No. 61307052).

REFERENCES

1. Hojo, H. and A. Mase, "Dispersion relation of electromagnetic waves in one dimensional plasma photonic crystals," *Plasma Fusion Res.*, Vol. 80, No. 2, 89–90, 2004.
2. Ginzburg, V. L., *The Propagation of Electromagnetic Wave in Plasma*, Pergamon, Oxford, UK, 1970.
3. Zhang, H. F., M. Li, and S. B. Liu, "Defect mode properties of magnetized plasma photonic crystals," *Acta Phys. Sin.*, Vol. 58, No. 2, 1071–1076, 2009.
4. Qi, L., Z. Yang, and T. Fu, "Defect modes in one-dimensional magnetized plasma photonic crystals with a dielectric defect layer," *Phys. Plasma*, Vol. 19, No. 1, 012509, 2012.
5. Hamidi, S. M., "Optcal and magneto-optical properties of one-dimensional magnetized coupled resoner plasma photonic crystals," *Phys. Plasma*, Vol. 19, No. 1, 012503, 2012.
6. Qi, L., "Photonic band structures of two-dimensional magnetized plasma photonic crystals," *J. Appl. Phys.*, Vol. 111, No. 7, 073301, 2012.
7. Zhang, H. F., S. B. Liu, X. K. Kong, B. R. Bian, and Y. N. Guo, "Dispersion properties of two-dimensioanl plasma photonic crystals with periodically external magnetic field," *Solid State Commun.*, Vol. 152, No. 7, 1221–1229, 2012.
8. Qi, L. and X. Zhang, "Band gap characteristics of plasma with periodically varying external magnetic field," *Solid State Commun.*, Vol. 151, 1838–1841, 2011.
9. Zhang, H. F., S. B. Liu, X. K. Kong, C. Chen, and B. R. Bian, "The characteristics of photonic band gaps for three-dimensional unmagnetized dielectric plasma photonic crystals with simple-cubic lattice," *Optic Commun.*, Vol. 288, 82–90, 2013.
10. Zhang, H. F., S. B. Liu, and X. K. Kong, "Photonic band gaps in one-dimensional magnetized plasma photonic crystals with arbitrary magnetic declination," *Phys. Plasma*, Vol. 19, No. 12, 122103, 2012.
11. Zhang, H. F., S. B. Liu, H. Yang, and X. K. Kong, "Analysis of band gap in dispersive properties of tunable three-dimensional photonic crystals doped by magnetized plasma," *Phys. Plasma*, Vol. 20, No. 3, 032118, 2013.
12. Zhang, H. F., S. B. Liu, and X. K. Kong, "Dispersion properties of three-dimensional plasma photonic crystals in Diamond lattice arrangement," *J. Lightwave Technol.*, Vol. 17, No. 11, 1694–1702, 2013.
13. Zhang, H. F., S. B. Liu, X. K. Kong, C. Chen, and B. R. Bian, "The properties of photonic band gaps for three-dimensional plasma photonic crystals in a diamond structure," *Phys. Plasma*, Vol. 20, No. 4, 042110, 2013.
14. Zhang, H. F., S. B. Liu, and B. X. Li, "The properties of photonic band gaps for three-dimensional tunable photonic crystals with simple-cubic lattices doped by magnetized plasma," *Optics & Laser Technol.*, Vol. 50, 93–102, 2013.

15. Zhang, H. F., S. B. Liu, and Y. C. Jiang, "The properties of photonic band gap and surface plasmon modes in the three-dimensional magnetized photonic crystals as the mixed polarized modes considered," *J. Plasma Physics*, doi:10.1017/S0022377814001238, 2014.